17th World Conference on Earthquake Engineering, 17WCEE
Sendai, Japan - September 13th to 18th 2020

SHEAR-STRAIN DEPENDENCY OF HIGH DAMPING RUBBER BEARING IN A SEISMICALLY ISOLATED BUILDING USING SEISMIC RECORDS

Y. Tobita [1], R. Nishiura [2], X. Wang [3], T. Hida [4], M. Nagano [5]

[1] *Structural Design Group, Asanuma Corporation, Tokyo, Japan, tobita-yoshinori@asanuma.co.jp*
[2] *Graduate Student, Tokyo University of Science, Chiba, Japan, 7114094@ed.tus.ac.jp*
[3] *Assistant Professor, Tokyo University of Science, Chiba, Japan, wangxin@rs.tus.ac.jp*
[4] *Assistant Professor, The University of Tokyo, Tokyo, Japan, hida@load.arch.t.u-tokyo.ac.jp*
[5] *Professor, Tokyo University of Science, Chiba, Japan, nagano-m@rs.noda.tus.ac.jp*

Abstract

It has been well known that high damping rubber bearings (HDB) can significantly reduce earthquake response of buildings, because input earthquake energy is consumed by their large deformation and high damping. The capacity of HDB is affected by the shear strain, which is one of the most influential dependencies in earthquake response. Loading tests of HDBs indicated that loading history must be taken into account to evaluate the capacity of HDBs. Dynamic properties of HDBs, such as the horizontal stiffness and equivalent damping ratio, are affected by cyclic-loading tests of HDB with large amplitude, empirical equations of which have been proposed. It is important to properly evaluate the shear-strain dependence of the stiffness of HDBs. The results are also effective to structural health monitoring using strong motions, which has been increased in recent years.

In this study, the shear-strain dependence of HDB of an exist building located in the southern part of the Tokyo Metropolitan area of Japan is examined based on observation records by system identification using the subspace method. The target building is a 6-story reinforced concrete residential building with HDB isolation layer at the base. Accelerometers are installed at the base of the isolation layer and the first floor. Records observed during the main shock and two aftershocks of the 2011 Great East Japan earthquake were used. It is found that, firstly, the shear stiffness of the HDB decreased depending on the magnitude of the experienced shear strain during the main shock. Then this stiffness marginally recovered in a short interval. During the aftershocks, the stiffness softening and recovering were repeated. Finally, it took approximately one month for the stiffness to recover completely. The earthquake response analysis is conducted based on modified models in which the experienced shear strain dependency is considered. The analysis results agreed well with the observation records. Therefore, it can be said that from earthquake response analysis, the effects of the experienced shear-strain dependency to earthquake response can be evaluated.

Keywords: Strong motion records, Seismically isolated building, High damping rubber bearing, Experienced shear strain dependency

1. Introduction

The design formula used to evaluate the stiffness of high-damping rubber bearings (HDBs) is based on shear strains of 10% or more, and the stiffness of HDBs cannot be accurately evaluated at strains below this level. In particular, the design formula for the horizontal stiffness of seismic isolators is set within a relatively large shear strain range, as its objective is to calculate the maximum response displacement experienced in a large earthquake. In many cases, there are no problems associated with the structural design. However, to study the response of a small amplitude such as environmental signals or railway vibrations, the accurate evaluation of the stiffness of the HDB for small shear strains is critical. The stiffness of HDBs at low shear-strain amplitudes can be evaluated using the Hardin–Drnevich (HD) model based on recorded observations [1,2]. HDBs are composed of a rubber material. Their responses are dependent on numerous parameters, such as signal amplitude, and they are subject to repetitive impact. The dynamic properties of HDBs such as the horizontal stiffness and equivalent damping ratio are influenced by the heating of the rubber via energy absorption during earthquake events. The shear-strain dependency of the HDB, which is induced by the Mullins effect of rubber, is critical to earthquake response based on the loading test results. The Mullins effect of rubber allows the softening of the stress–strain curve, which occurs when a load exceeds the all-time maximum value. It is therefore necessary to evaluate the influence of the maximum shear strain on the earthquake response [3].

This paper presents the detection results for the frequency of the HDB using a system identification method based on the subspace method, in addition to the investigation of the maximum empirical strain with respect to their variations based on actual building seismic records.

2. Overview of the Building and Seismic Observations

2.1 Overview of the building

The building under consideration is located in Zushi City at the northern Miura Peninsula in Japan (see Fig. 2, afterwards). Table 1 summarizes an overview of the target building. Fig. 1 shows the plan of the first floor and a cross section of the ground including the piles. The building is a six-story residential housing complex built with reinforced concrete. The long side of the building (noted as EW in this paper) is a rigid frame structure, whereas the short side (noted as NS) is a rigid frame structure with a shear wall. The building is a base-isolated structure; base isolation devices are placed between the first floor and the basement. The upper structure is split into buildings A and B by an expansion joint in the middle of the long side. The following evaluation concerns the building B. The dimensions of the building B are 74.2 m × 15.9 m.

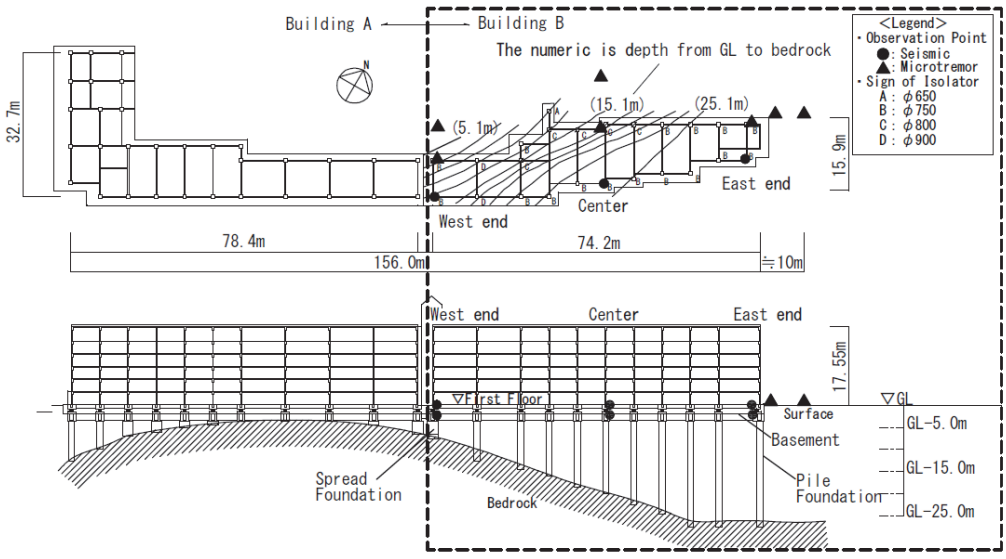

Fig. 1 – Plan and cross-sectional schematics of the building and seismic observation points

Table 1 – Overview of the target building.

Location	Zushi City, Kanagawa prefecture, Japan		
Use	Residential housing		
Construction Area	958.6 m^2	Standard floor area	692.6 m^2
Number of Floors	6 floors	Height	17.55 m
Upper Structure	Reinforced concrete (Basement: seismically isolated structure)		
	Long side: rigid frame structure	Short side: rigid frame structure with a shear wall	
Foundational Structure	Combination of a spread foundation and cast-in-place concrete piles		

Table 2 – Properties of the isolator (high damping rubber).

Type of isolator	**HM065H6**	**HM075H6**	**HM080H6**	**HM090H6**
Symbol in Fig. 1	A	B	C	D
Outer diameter (mm)	650	750	800	900
Effective area (mm^2)	3240	4339	4850	6185
Total rubber thickness (mm)	162		160	
Shear modulus G (N/mm^2)	1.81 (Shear strain $\gamma = 0.1$)			
Horizontal stiffness K_h (N/mm)	36.30	48.61	55.01	70.15
Number of isolators	1	16	5	2

2.2 Overview of the base isolation devices

Twenty-four HDBs are installed as base isolation devices. Fig. 1 shows the placement of the base isolation devices. Table 2 lists the properties of the isolators. The total thickness of each HDB is 160 or 162 mm, and their diameters vary from 650 to 900 mm. Seismic isolation bearings are placed so that the their center of rigidity match with that of the upper structure. In the structural design, the natural periods in NS direction from an eigen analysis are 1.66 and 2.83 s at shear strain levels of 10% and 100% in the HDB, respectively.

2.3 Outline of the seismic observations

The observation points of the strong motions are marked as filled black circles in Fig. 1. In total, six seismic observation points are located at the west end, center, and east end in the basement and on the first floor. Seismic observations are carried out in both the horizontal (EW, NS) and vertical (UD) directions at the center and along the short sides (NS) at both ends of the building. The seismic observations are obtained in the range of 0.1–30 Hz with a sampling frequency of 100 Hz; the seismograph has a maximum amplitude of 10 m/s^2.

3. Target Earthquakes and Strong Motion Records

In total, the records of 130 earthquakes were obtained at the building between April 2000 and April 2018. Fig. 2 presents the relationship between the locations of the hypocenters and the observation sites. With reference to the recorded observations, the earthquake with the highest acceleration was the Great East-Japan earthquake (Tohoku Earthquake, 2011) that occurred at 2:46 p.m. on March 11, 2011, referred to as M0311A. In this event, the maximum acceleration observed at the building was 81.97 cm/s^2. However, the building and foundation were not subject to damage. Table 3 presents the overview of the target earthquakes. Fig. 2 presents accelerograms during the M0311A earthquake; the M0311B earthquake that occurred approximately 30 min later; and the M0411A earthquake that occurred after approximately 1 month later, off

the coast of the Miyagi prefecture. The M0311B and M0411A earthquakes were aftershocks of the M0311A earthquake. Further, an earthquake with a small amplitude was observed between M0311B and M0411A. The amplitude of earthquake M0311A gradually increased for approximately 130 s after its onset , and then decreased. The duration of the earthquake was approximately 450 s, which was longer than those of other recorded ground motions at the site. This significant motion decreased the stiffness of the isolator below its initial stiffness. Consequently, the predominant ground-motion period on the first floor became longer. The maximum accelerations of M0311B and M0411A were approximately a 50% and 25% that of M0311A.

Fig. 3(a) presents acceleration response spectra at the first floor to the basement. Fig. 3(b) presents the transfer function of the first floor to the basement including that of the micro-tremor measurements carried out in May 2017. Fig. 3 (a) presents the predominant frequencies of the basement when the M0311A and M0311B earthquakes were at approximately the same frequency, although their seismic amplitudes were significantly different. In comparison, the predominant frequency of the basement subject to M0411A was 2.0 Hz, which indicates that the seismic signal contained several short-period components. Fig. 3 (b) reveals that the predominant frequency of the first floor (upper-seismic isolation layer) was 1.31 Hz in very small amplitude ranges. In general, the predominant frequency is higher if HDB stiffnesses are higher during earthquakes with small acceleration (displacement) amplitudes. However, the predominant frequencies of M0311A and M0311B, which differed significantly with respect to acceleration, were almost the same. This indicates that the seismic isolation layers exhibited almost the same stiffness during the earthquakes. Moreover, in comparison, the predominant frequency of the first floor when subject to M0411A was 0.9 Hz, which indicates an increased stiffness of the seismic isolation device.

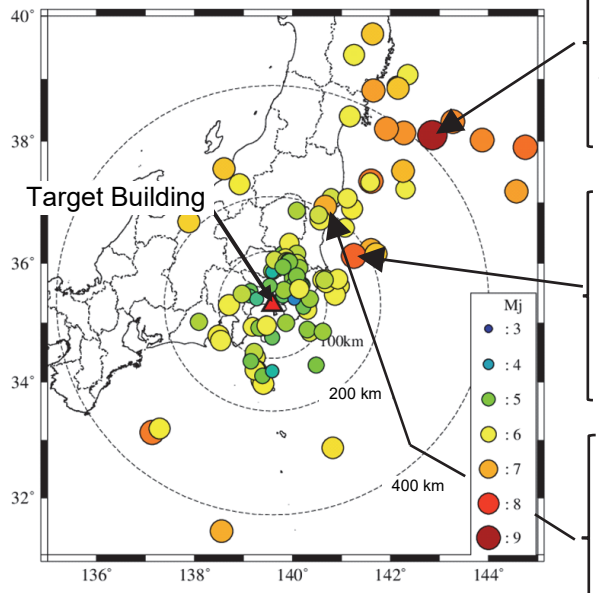

Fig. 2. (A): Location of observed earthquake hypocenters to target building

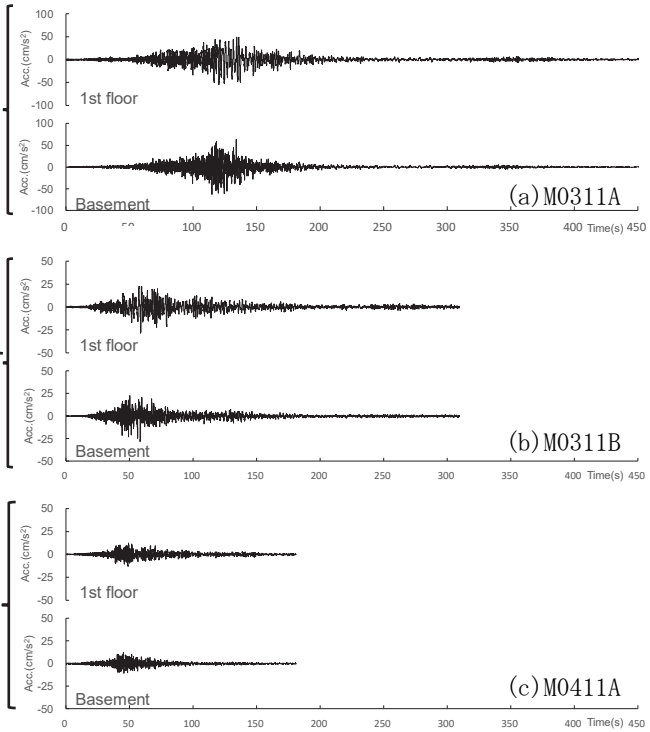

Fig. 2. (B): accelerograms of the target earthquakes

Table 3– Overview of the target earthquakes

Sign of Eq.	Observation Date Time	Location	Magnitude	Distance of Epicenter (km)	Maximum Acc. (cm/s^2)	Time Interval	Temperature (℃)
M0311A	2011.03.11 14:47:47	East of the Oshika Peninsula of Tōhoku	9.0	438	63.31	–	11.2
M0311B	2011.03.11 15:16:17	East of Ibaraki pref.	7.7	199	27.59	29 min.	11.0
M0411A	2011.04.11 17:16:58	Hamadōri region of Fukushima	7.0	186	11.97	31 Days	17.3

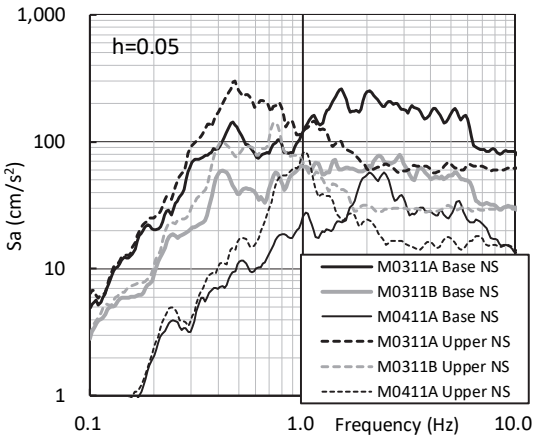

Fig. 3(a) Response spectrum

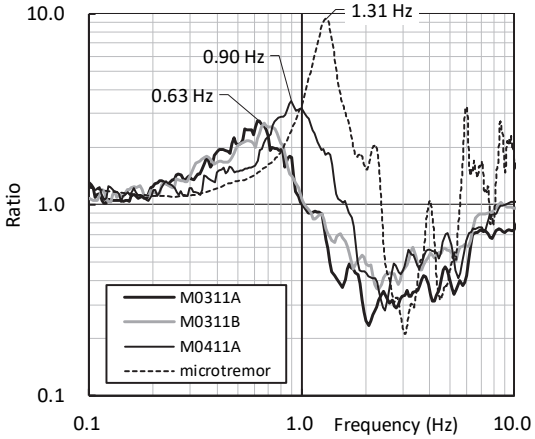

Fig. 3(b) Transfer function of first floor to basement

4. Dynamic Building Properties Based on System Identification

4.1 System identification using M0311A records

An identification method is generally employed for the calculation of the natural frequency and damping factor of a structure based on observations of significant motion. This section describes the natural frequency and damping factor of the target building based on recorded seismic observations during the 2011 Tohoku earthquake. Fig. 4 presents the changes in the frequency and attenuation constants with respect to time, as determined using the identification method. These response characteristics of the building were evaluated through the subspace state space system identification (4SID) method [4]. This figure reveals that the frequency at the start time was 1.39 Hz, then fell to 0.6 Hz at time of the maximum amplitude, before reaching a final value of 1.09 Hz. The final natural frequency was lower than the initial frequency by a factor of approximately 0.82. The initial damping factor was approximately 2.5%, and it increased to nearly 20% in association with the increased relative displacement of the isolator.

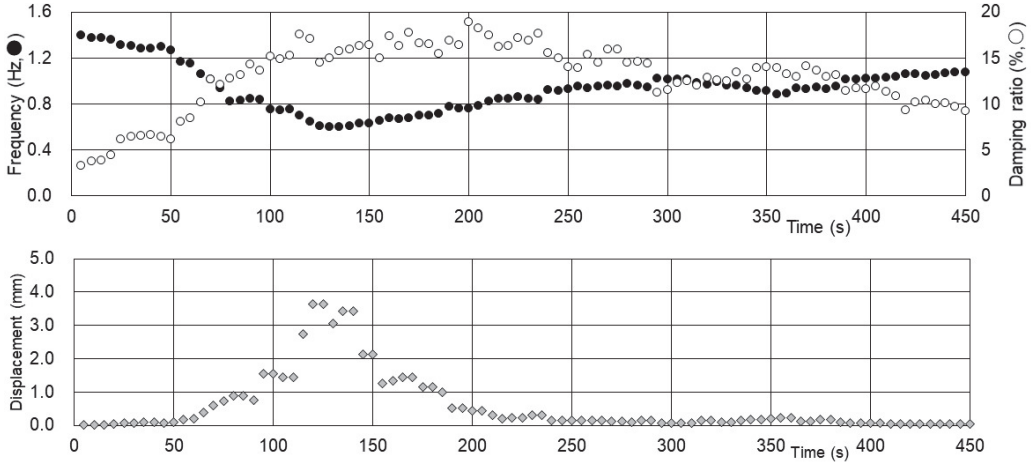

Fig. 4 Temporal variation of natural frequency and damping factor (M0311A)

4.2 Natural frequency recovery ratio

Fig. 5 presents the consecutive accelerograms of the observed earthquakes (M0311A, M0311B, M0315A, and M0411A) and the temporal variations of the detected natural frequencies. Approximately 30 min after the main shock (M0311A) of the abovementioned Tohoku earthquake, there was an M7.7 aftershock

(M0311B) off the east-coast of Ibaraki prefecture, and M0411A occurred 1 month later after several subsequent earthquakes. For the observed ground motions, the strain dependence of the frequency (shear stiffness) was investigated using the system identification method. Fig. 5 presents the changes in frequency due to each ground motion with respect to time. The horizontal axis in the figure represents time (broken scale), and the vertical axis represents the frequency. As mentioned above, the initial frequency of M0311A was 1.39 Hz, which decreased in association with the increase in amplitude, and then increased to a final frequency of 1.09 Hz. Thereafter, the initial frequency of M0311B was 1.14 Hz, which slightly increased, and then decreased in accordance with an increase in amplitude, thus reaching a final frequency of 1.09 Hz. It was found that, the initial shear stiffness of the HDBs during M0311B decreased depending on the magnitude of the experienced shear strain during the main shock(M0311A) based on observation records. After 1 month, the initial frequency of M0411A was almost the same as the initial frequency of M0311A. However, at end of the ground motion, the natural frequency was lower than it was at the end of M0311A. Hence, the frequency of the HDB was found to vary constantly and significantly with respect to the amplitude and oscillation period of the earthquake.

Fig. 6 presents the relationship between the time elapsed from the start of the earthquake and the recovery ratio as proposed by Kitamura et al. [5]. The horizontal axis represents the time elapsed (units: min) from the beginning of M0311A, and the vertical axis represents the ratio of the frequency to the initial frequency of M0311A. The figure reveals that the approximate formula of the recovery rate obtained by the experiment is consistent with the observed values, and thus, the formula can be employed to obtain accurate recovery ratio estimates.

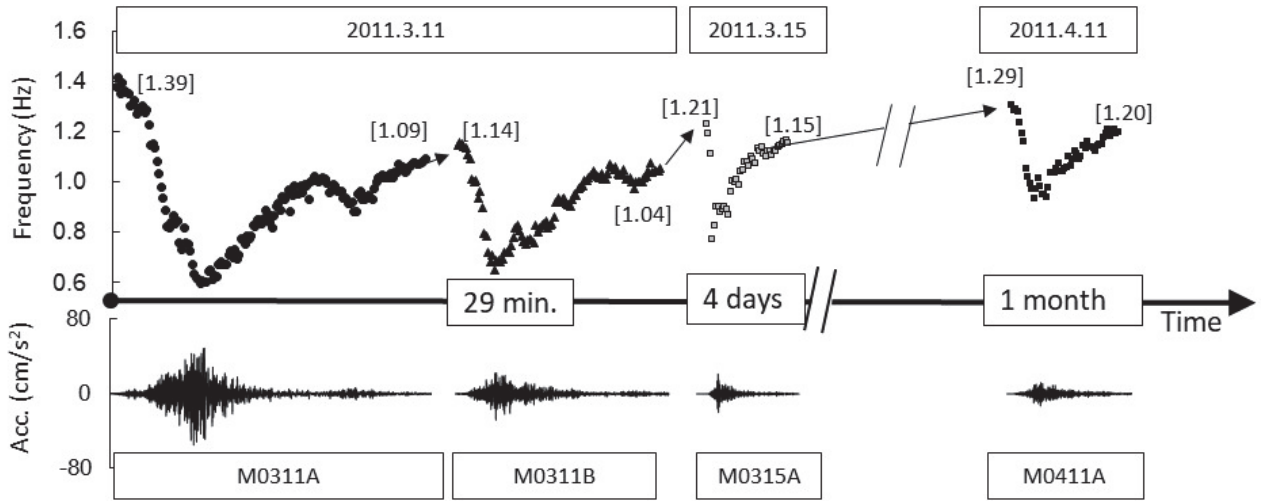

Fig. 5 Acceleration with respect to time of observed seismic signal and natural frequencies as determined through system identification based on the subspace method.

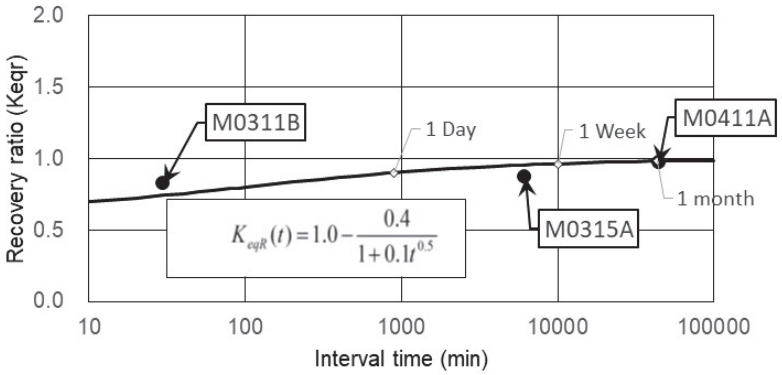

Fig. 6 Recovery ratio of equivalent shear stiffness with respect to interval time

4.3 Dependence of shear strain on stiffness of seismic isolation layer

Fig. 7 presents the relationship between the shear strain and stiffness ratio of the base-isolated layer during an earthquake. The horizontal axis represents the assumed shear strain of the seismic isolation device (γ: relative displacement; thicknessof the rubber layer of the seismic isolation device = 161 mm), and the vertical axis represents the ratio of the square of the frequency at the initial strain (1.39 Hz). It was assumed that the square of the frequency is proportional to the shear stiffness. As can be seen from the figure, between the start of the earthquake to the point at which maximum shear strain was reached, the identified point is indicated by the black symbols; and after the maximum shear strain, the identified point is indicated by the gray symbols. Further, different symbol shapes indicate different earthquakes. The analysis was conducted using the HD model in the same manner as in Tobita et al. [2]; i.e., G/Go-γ is expressed by Equation (1), and the resulting curve is shown in Fig. 7.

First, the stiffness decreased over time , until after the maximum stress was reached, after which the stiffness began gradually recovering

First, the points (infilled black circle) within the time-period of 0–150 s when the maximum displacement of M0311A occurred were consistent with the line (Eq.1; *Kr-γ*) generated using the HD model, that is , the stiffness decreased over time, until after the maximum stress was reached, after which the stiffness began gradually recovering. Thus, the stiffness of the seismic isolator at a small amplitude can be evaluated using the HD model with the shaking experiment results. It can be expressed as follows:

$$K_{\mathrm{r}} = \frac{K_{\mathrm{eq}}(\gamma)}{K_{\mathrm{eq}}(\gamma=100\%)} = \frac{\alpha}{\left(1+\frac{\gamma}{\gamma_{0.5}}\right)} \tag{1}$$

where γ is the shear strain, and $\gamma_{0.5}$ is the shear strain when the shear stiffness is reduced by 50%. The evaluation curve reveals that when the shear strain was reduced by 50%, the strain (γr) due to M0311A was 4%. The stiffness was almost coincident with the value obtained in [2], the maximum shear strain of the seismic isolation layer was approximately 20%, the ratio of stiffness at that time was 0.20–0.25, and the stiffness was approximately 1/4 of the initial value. However, the stiffness from 150–450 s after the maximum displacement (as indicated by the solid gray circles in Fig. 7) was in good agreement with the line that was reduced by a factor of 0.6. In the case of M0311B (represented by solid black triangles), the initial stiffness of the seismic isolation layer recovered slightly compared to the final stiffness during M0311A, and it was approximately 0.7Keq. However, the stiffness after the maximum displacement (solid triangle in gray) was 0.6Keq. Thereafter, the building was subject to several seismic ground-motions; and the initial stiffness at the start time of M0411A, after approximately a month of recovery, was approximately 0.9 Keq (solid black squares). The maximum strain was 2.5%, and the final stiffness was 0.7 Keq (solid gray squares).

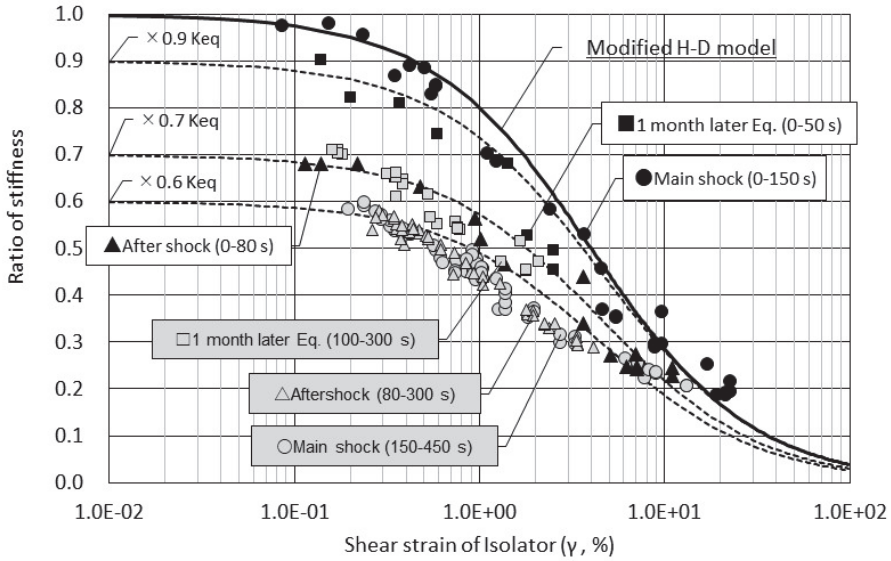

Fig. 7 – The relationship between with the strain and the stiffness of the isolator

Therefore, the stiffness of the HDB after experiencing maximum deformation during the earthquake was lower than the initial stiffness due to the maximum empirical strain (Mullins effect) according to seismic observations.

5. Response Analysis Considering Stiffness with Strain Dependence of HDBs

Consecutive earthquakes, e.g., M0311A and M0311B, have a more significant influence on the frequencies of seismically isolated buildings supported by HDBs than do single seismic waves. This section describes the effect of continuous ground motion on seismic responses based on a seismic response analysis that considered the strain dependence of HDB stiffness. The analysis models were as follows: a two-dimensional FEM model was used for ground-motion evaluation, and a three-dimensional frame model was used to represent the building structure, including the piles and seismic isolation layers[1]. The restoring force properties of the seismic isolation layer were estimated using a multiple linear model based on the skeleton curve of the HD model. The initial damping constant was 2% for the superstructure and seismic isolation layer, as determined by the identification results. The nonlinear hysteretic model used to calculate an appropriate solution based on the seismic response analysis requires the variations in stiffness denpending on the amplitude. However, these variations is complex. In this study, the stiffness of the seismic isolation layer was evaluated base on changes in the stiffness before and after the occurrence of the maximum amplitude. Fig. 8(a) presents the results of the seismic response analysis using the stiffness formula expressed in Equation (1), which was in relatively good agreement with the recorded observations for 0–140 s of M0311A. However, after the maximum displacement (140 s), there was a slight error in the period following the maximum amplitude. Fig. 8(b) presents the analysis results when the stiffness was set as 0.6Keq after 140 s, which was almost completely in agrreement with the observation records. Similarly, Fig. 9(a) presents the results of the seismic response analysis of the M0311B aftershock based on the stiffness formula expressed by Equation (1). As mentioned above, the stiffness of the seismic isolation device was reduced; thus, an error was observed with respect to the period after the maximum aftershock. In the case where the equivalent stiffness was reduced to 0.7 Ko from 0 to 140 s and to 0.6 Ko afterwards, the calculated structural response was in good agreement with the recorded observations, as shown in Fig. 9(b). Therefore, the seismic response analysis was effective for the evaluation of consecutive earthquakes with consideration of the empirical strain.

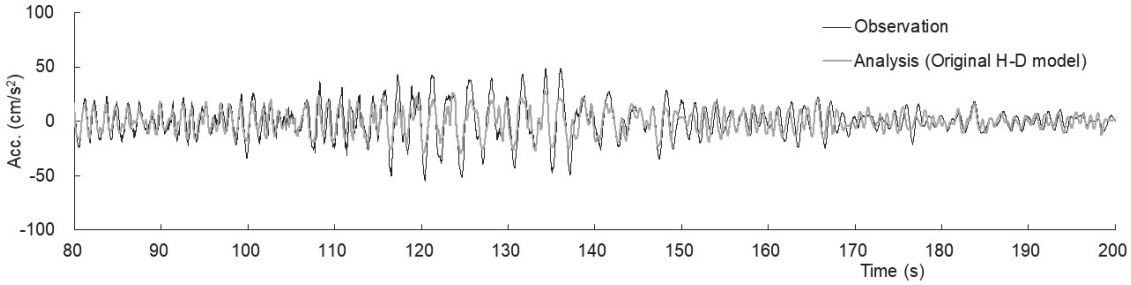

(a) Results using the stiffness of the original model

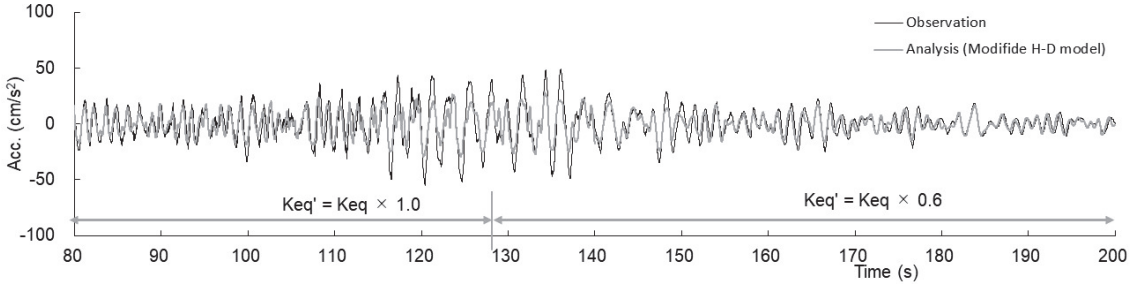

(b) Results using the modified stiffness

Fig. 8 – Comparison of time history results considering stiffness with strain dependence (M0311A, main shock)

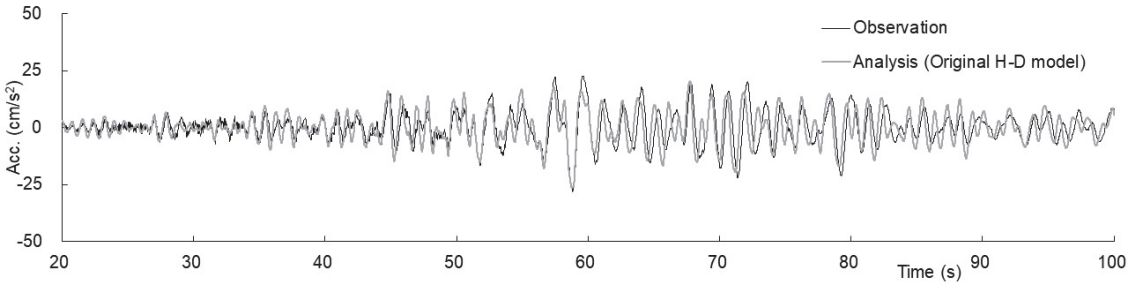

(a) Results using the stiffness of the original model

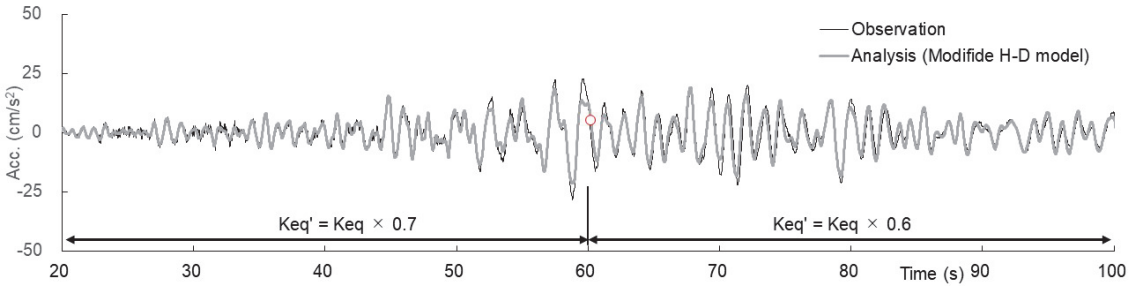

(b) Results using the modified stiffness

Fig. 9 – Comparison of time history results considering stiffness with strain dependence (M0311B, aftershock)

6. Conclusion

The system identification method was employed for the earthquake motions observed in the target building during the Great East-Japan Earthquake that occurred on March 11, 2011. Moreover, changes in the frequency and damping constant based on the observed earthquake motions were reported, in addition to the relationship between the shear stiffness and the shear strain of the building's base-isolation device. Furthermore, the aftershocks observed 30 min and approximately 1 month after the main shock were examined,, and the recovery rate of the shear stiffness of the base-isolation device was described. Hence, the following conclusions were reached.

1) The stiffness of HDB subjected to earthquake motion decreases in accordance with an increase in the amplitude (shear strain), and the relationship between the strain and the decrease in stiffness can be evaluated using the HD model.
2) The shear stiffness of HDB is different before and after the earthquake when subject to a relatively large seismic amplitude. Thereafter, a decrease trend was observed when compared with the rigidity, up to the maximum value. Moreover, it was found to be dependent on the amplitude and maximum shear strains.
3) The results based on the observation records revealed that the damping constant of the HDB was initially 2–3% larger than that estimated at the design phase, accounting for an approximately 20% difference in the maximum displacement.
4) The decrease in the shear stiffness of the HDB due to a relatively large earthquake does not recover within several hours. Moreover, gradual recovery of the shear stiffness was observed. In particular, approximately 1 month is required for complete recovery.
5) The results of the seismic response analysis using the strain-dependentHD model for the HDBs were in good agreement with the recorded observations. This verifies the effectiveness of the model for the seismic response analysis of consecutive earthquakes under the consideration of the empirical strain dependency.

7. Acknowledgements

We greatly appreciate the cooperation of the residents of the buildings during the microtremor measurements. Graduate and undergraduate students at Tokyo University of Science assisted with the microtremor measurements and the analyses of the compiled ambient vibration data.

8. References

[1] Y. Tobita et al. (2019): Seismic response analysis of seismically isolated building constructed on soil with inclined bedrock based on strong motion records and evaluation of pile stresses, *AIJ Journal of Technology and Design*, *Vol.17, No.36*, pp.149-159 (in Japanese)

[2] Y. Tobita, M. Nagano, H. Kitamura, T. Sato, K. Suzuki, Y. Matsuda, T. Yamauchi, and H. Uebayashi (2018) : Dynamic characteristics of a seismically isolated building on soil with inclined bedrock using ambient vibration and strong motion records, *16th European Conference on Earthquake Engineering, ID10507*

[3] O. Yasuki et al. (1995): Effect of experienced shear strain dependency of high damping rubber bearing on earthquake response of isolation structure, *AIJ Journal of Technology and Design, No.472*, pp.75-84 (in Japanese)

[4] M. Verhaegen and P. Dewilde (1992): Subspace model identification, Part 1: The output-error state-space model identification class of algorithms, *International Journal of Control, 56 (5)*, pp.1187-1210.

[5] H. Kitamura et al. (2010): Evaluation of the influence of heat-mechanics interaction behavior in high-damping rubber bearings on seismic response of base-isolated buildings, *AIJ Journal of Technology and Design, Vol.75, No.655*, pp.1635-164 (in Japanese)

